Award Number: W81XWH-11-1-0531

TITLE: Radiation-Induced Vaccination to Breast Cancer

PRINCIPAL INVESTIGATOR: William H. McBride

CONTRACTING ORGANIZATION: University of California at Los Angeles,
Los Angeles, CA 90024

REPORT DATE: December 2016

TYPE OF REPORT: Final

PREPARED FOR: U.S. Army Medical Research and Materiel Command
Fort Detrick, Maryland 21702-5012

REPORT DOCUMENTATION PAGE		Form Approved OMB No. 0704-0188

1. REPORT DATE *(DD-MM-YYYY)*	2. REPORT TYPE	3. DATES COVERED *(From - To)*
December 2016	FINAL	30 Sep 2011 - 29 Sep 2016

4. TITLE AND SUBTITLE	5a. CONTRACT NUMBER
Radiation-Induced Vaccination to Breast Cancer	5b. GRANT NUMBER W81XWH-11-1-0531
	5c. PROGRAM ELEMENT NUMBER
6. AUTHOR(S) William H. McBride	5d. PROJECT NUMBER
	5e. TASK NUMBER
	5f. WORK UNIT NUMBER
7. PERFORMING ORGANIZATION NAME(S) AND ADDRESS(ES) University of California at Los Angeles Los Angeles, CA 90024	8. PERFORMING ORGANIZATION REPORT
9. SPONSORING / MONITORING AGENCY NAME(S) AND ADDRESS(ES) U.S. Army Medical Research And Materiel Command Fort Detrick, MD 21702-5012	10.SPONSOR/MONITOR'S ACRONYM(S)
	11. SPONSOR/MONITOR'S REPORT NUMBER(S)

12. DISTRIBUTION / AVAILABILITY STATEMENT
Approved for public release; distribution unlimited.

13. SUPPLEMENTARY NOTES

14. ABSTRACT Inhibiting TGFβ in the context of focal irradiation seems to create a favorable systemic immune landscape that drives T cell memory differentiation while limiting myeloid suppression.

15. SUBJECT TERMS

16. SECURITY CLASSIFICATION OF:			17. LIMITATION OF ABSTRACT	18. NUMBER	19a. NAME OF RESPONSIBLE PERSON
a. REPORT U	b. ABSTRACT U	c. THIS PAGE U	UU	43	19b. TELEPHONE NUMBER *(include area code)*

Standard Form 298 (Rev. 8-98)

Table of Contents

1 Introduction

The biology of TGFβ is very complex owed to the diversity in signal interpretation, especially in the cancer setting where it affects tumorigenesis, metastatic potential, tumor immune interaction and resistance to therapy. Of the 3 mammalian TGFβs currently known, the best characterized is TGFβ1. It is secreted as a large latent complex bound to latency-associated protein (LAP) and latent TGFβ binding protein (LTBP). Only TGFβ released from this complex is able to bind the high-affinity tetrameric receptor complex made of type I and type II dimers that signal through serine/threonine kinase domains and Smad proteins to affect cellular growth, differentiation and morphogenesis. Various negative feedback regulatory pathways exist through inhibitory iSmads, Smad 7, competitive receptor binding, or receptor degradation. In addition, complex cross-talk exists between Smads and Smad-independent signaling pathways, especially mitogen activated protein kinase (MAPK) pathway and PI3K kinase pathways, which leads to both synergistic and antagonist interactions. It is this cross-talk that explains the diverse and even paradoxical physiological and pathological observations often ascribed to TGFβ.

Originally identified as a soluble factor inducing neoplastic transformation, of relevance to this study, TGFβ can also potently inhibit proliferation of epithelial tumor cells and the immune system. Some cancers mutate to escape the suppressive effects of TGFβ on proliferation, while others remain responsive. A radioresistant cancer phenotype can result, including in breast cancer, and inhibition of TGFβ can enhance radiation-induced DNA damage that translates into a greater tumor growth delay in vivo (1). In the immune system, TGFβ is a key suppressor dampening macrophage and lymphocyte proliferation and activation and maintaining immunological homeostasis. It is therefore not surprising that the TGFβ signature is a shared trait in a subgroup of breast cancer patients who all fail to benefit from protective immune responsiveness (2).

In this pilot study we used a human IgG4 monoclonal antibody (Fresolimumab, GC1008, Genzyme, Cambridge, MA) that binds and neutralizes all mammalian isoforms of TGFβ (1,2 and 3). Metastatic breast cancer patients received a combination of focal hypofractionated irradiation of selected tumor metastases along with systemic TGFβ blockade. The primary objectives were to assess safety, feasibility, and abscopal tumor regression and to monitor immune responses in these patients. The abscopal responses were assessed by imaging. The UCLA component was 3 fold: 1) to enroll patients into the clinical trial, 2) to assess immune responses using blood samples before, during and after treatment by multi-channel flow cytometry for immune monitoring, 3) to examine the effects of targeting TGFβ on the activities and numbers of breast cancer stem cells with and without irradiation. All 3 aims have now been completed and the publications for Fresolimumab effects that incorporate immune monitoring results with patient outcome data are being finalized. Publications from other aspects of the UCLA efforts have previously been submitted.

Since Fresolimumab was discontinued as a drug by the manufacturer, we switched -with DOD approval- to the small molecule TGFβ inhibitor, LY2157299 monohydrate (Galunisertib, Eli Lilly). UCLA opened the trial for accrual under this new protocol (Clinical trials identifier # NCT02538471) but with no accrual due to competition from other trials using checkpoint inhibitors that have entered the clinic with some

success since our trial was initiated. It is unlikely that this situation will change in the near future. We therefore present here excerpts from the proposed publication on immune monitoring that we expect to submit in the near future.

2 Body

2.1 Methods

2.1.1 Patients, treatment & sample collection

Blood samples came from 22 patients with metastatic breast cancer undergoing treatment with Fesolimumab and hypofractionated radiation therapy at the New York University School of Medicine (n=15) and at the David Geffen School of Medicine, University of California, Los Angeles (n=7) with local IRB approval and consent (Trial registration at clinicaltrials.gov under #NCT01401062). Patients with at least three distinct metastatic sites were randomized into two study arms receiving the TGFβ-neutralizing human monoclonal antibody Fresolimumab (GC1008, Genzyme, Cambridge, MA) at a dose of either 1mg/kg GC1008 or 10mg/kg GC1008 i.v. every three weeks for a total of five cycles (week 0, 3, 6, 9 and 12, Figure 1A). After the first cycle, external beam radiation of 7.5Gy was given consecutively on Monday, Wednesday and Friday to one metastatic site for a total of 22.5Gy (week 1). Radiation treatment was repeated to a second metastatic site after 3 cycles of antibody treatment (week 7). The third metastatic site was not targeted by radiation and used as a barometer for potential systemic anti-tumor effects.

Up to 60ml of blood was drawn into heparinized BD vacutainer® tubes (BD, Franklin Lakes, NJ) at baseline, after the first cycle of antibody infusion and radiation (week 2), after the second cycle of antibody infusion (week 5) and after completion of treatment (week 15). Peripheral blood mononuclear cells (PBMCs) were isolated by gradient centrifugation within 3h of blood draw and controlled-rate frozen in aliquots in human AB serum containing 10% (v/v) DMSO at -80°C before transfer to liquid nitrogen until further use. Additionally, a SST serum tube and a CTAD plasma tube were also drawn and processed according to manufacturers recommendation before storage in aliquots at -80°C. Batches of frozen PBMCs, serum and plasma were shipped between UCLA and NYU overnight on dry ice. PBMCs from 11 healthy volunteers were isolated on Ficoll-Paque Premium™ at UCLA as above and served as controls.

2.1.2 Thawing

Serial samples of individual patients were assayed on the same day for tetramer/dextramer binding and levels of lymphoid and myeloid markers (see below). PBMCs from patients and healthy subjects were thawed by dilution in pre-warmed RPMI-1640 medium with 10% (v/v) FBS. Cells were treated with DNAse, washed and re-suspended at $1x10^6$ cells/ml in PBS.

2.1.3 HLA-A2 testing and Dextramer-binding assay

HLA-A*0201 positivity was confirmed by staining $1\text{-}2x10^5$ PBMCs in 2% FBS/PBS staining buffer (BD Pharmingen, San Diego, CA) with 1µl of BB515 anti-HLA-

A2 antibody for 30 minutes at 4°C, subsequent washing, resuspension in 300µl PBS and analyses by flow cytometry (LSRFortessa; BD Biosciences, San Jose, CA). Cells from a single healthy volunteer with confirmed HLA-A*0201^{+} status served as staining control at all times (internal control).

1x10^{6} aliquots from HLA-A*0201-positive subjects and the internal control were prepared with fixable viability stain 510 (BD Horizon) according to manufacturers instructions prior to incubation with 10µl of the MHC dextramer-PE for the HLA-A2-restricted survivin epitope Sur1M2 (LMLGEFLKL)(3) (Immudex, Copenhagen, DK) in 5% FBS/PBS. Alternatively, a tetramer with the identical survivin epitope (Beckman Coulter, Fullterton, CA) (4) was used. Sample volume permitting, an additional 1x10^{6} aliquot was stained with a MHC dextramer mix containing 10µl of each of the HLA-A2-restricted epitopes for Jarid1B (QLYALPCVL-FITC), Mucin-1 (STAPPVHNV-PE) and Her2/neu (KIFGSLAFL-APC) (5-7). After an initial 10 minutes room temperature incubation with the dextramers, 4µl PerCP-Cy5.5 anti-CD8 (clone RPA-T8) was added to each sample for an additional 20 minute incubation on ice before washing in 5% FBS/PBS and subsequent flow cytometric analysis. PBMCs from a single HLA-A*0201-positive volunteer were run alongside as an internal control for each assay. 2-3x10^{5} events were accumulated. The gating strategy was: 1) SSC-A/FSC-A dot plot to set lymphocyte gate; 2) FSC-H/FSC-A dot plot to exclude doublets; 3) FVS510-A/FSC-A dot plot to set viability gate**;** 4) CD8/FSC-A dot plot to set gate for CD8^{high} lymphocytes, excluding NK cells (CD8^{low}) and 5) Dextramer/CD8 dot plot to select dextramer^{+} CD8 lymphocytes. Quality control required ≥10,000 viable events and ≥2,000 CD8^{+} T cells.

The arbitrary nature of the dextramer/tetramer CD8^{+} gate was addressed by setting a consistent 0.03% lower limit according to the historic binding of the negative tetramer to the internal control (4, 8). The resulting average positivity of this control sample reached 0.122% ± 0.082 survivin reactive CD8+ T cells which was also adopted for dextramer staining.

2.1.4 Lymphoid and myeloid panels

1-2x10^{6} aliquots of PBMCs from all subjects, regardless of the HLA-A*0201status, were prepared with fixable viability stain 510, as above, prior to assaying for surface markers. PBMCs from one volunteer served as an internal control for each assay (see above).

The lymphoid panel was premixed in brilliant stain buffer (BD Horizon/BD Biosciences) containing FITC anti-human CD4, PE anti-human CD25, PE-CF594 anti-human CXCR3, PerCP-Cy5.5 anti-human CD3, PE-Cy7 anti-human CD127, APC anti-human CD45RA, Alexa Flour 700 anti-human CD8, BV421 anti-human PD-1 and BV650 anti-human CCR6. For most samples, 1-2x10^{6}cells were stained in 50µl 2% FBS/PBS staining buffer (BD Pharmingen, San Diego, CA) for 20 minutes at room temperature following a 10 minute pre-heat activation at 37°C in the presence of BV605 anti-human CCR7 alone. Cell were washed and re-suspended in 300µl of PBS and analyzed by flow cytometry within 2 hours. If possible, 1-2x10^{5} events were accumulated on a LSRFortessa (BD Biosciences, San Jose, CA) with UltraComp eBeads compensation (eBioscience, Inc., SanDiego, CA). Analysis was done with FlowJo, LLC (Ashland, OR) using the following gating strategy: 1) FSC-H/FSC-A dot

plot to exclude doublets; 2) FVS510-A/FSC-A dot plot to set viability gate**;** 3) SSC-A/FSC-A dot plot to gate in lymphocyte; 4) CD3/FSC-A dot plot to set gate for $CD3^+$ T cells; 5) CD8/CD4 dot plot to select $CD3^+CD8^+$ and $CD3^+CD4^+$ T cells; 5) $CD3^+CD8^+$ and $CD3^+CD4^+$ T cells where individually checked for CCD7/CD45RA expression to dissect naïve, effector, central memory and effector memory subsets (Maeker et al. 2012) as well as for their PD-1 levels; 7) Regulatory T cells (Tregs) were defined within the $CD3^+CD4^+$ T cells gate according to $CD25^{hi}$ $CD127^{lo}$ status while the combination of CXC3 and CCR6 guided the distinction between T helper lineages. Quality control required all acquired data to be ≥50% viability and ≥2,000 $CD3^+CD8^+$ and $CD3^+CD4^+$ T cells.

The myeloid panel comprised FITC anti-human HLA-DR, PE anti-human CD14, PE-CF594 anti-human CD56, PerCP-Cy5.5 anti-human CD11b, PE-Cy7 anti-human CD19 , APC anti-human CD15, Alexa Flour 700 anti-human CD11c, APC-H7 anti-human CD20, BV421 anti-human CD123, BV510 anti-human CD3, and BV650 anti-human CD16 premixed in brilliant stain buffer as above. 1-2x10^6cells were stained in 50µl 2% FBS/PBS staining buffer for 30 minutes at room temperature, washed and analyzed as above. The gating strategy was as follows: 1) FSC-H/FSC-A dot plot, gating out doublets; 2) 510-A/FSC-A dot plot to exclude $CD3^+$ lymphocytes and dead cells**;** 3) CD19/FSC-A dot plot to select live $CD3^-CD19^-$ and live $CD3^-CD19^+$ cells with the $CD19^+$ subset ultimately enumerating B cells based on simultaneous CD20 expression; 4) The $CD19^-$ subset was used to distinguish between HLA-DR^+ and DR^- myeloid lineages; 6) DR^+ cells led to monocytes and dendritic cells (DCs) subsets according to CD14/CD16 expression for classical, intermediate and non-classical monocytes and $CD11c^{hi}/CD14^-$ and $CD123^{hi}/CD14^-$ for myeloid DCs and plasmacytoid DCs, respectively; 7) DR^- cells on the other hand led us to $CD14^-$-gated $CD56^+CD16^{+/-}$ NK cells and $CD11b^+CD15^{hi}$ granulocytic myeloid-derived suppressor cells (gMDSC) as well as $CD14^+CD16^-$ monocytic myeloid-derived suppressor cells (mMDSC) (Maeker et al. 2012).

2.1.5 Plasma levels of tryptophan and kynurenine

The method to quantify tryptophan and kynurenine was adapted from previous work by Midttun et al. (9). Solutions of internal standards, namely 500pmol 2H5-kynurenine and 2nmol 2H3-tryptophan, both in 10µL of water, were added to 100µl aliquots of plasma and vigorously mixed. Samples were then treated with 300µl methanol, vigorously mixed again followed by a 30 minute incubation at RT. After a 5 minute centrifugation at 16,060 x g the supernatants were transferred to clean microcentrifuge tubes and dried in a vacuum centrifuge. Dilute hydrochloric acid (0.1N, 100µL) was added to the dried residues and then vigorously agitated. These samples were centrifuged again for 5min at 16,060 x g (RT) and supernatants transferred to LC injector vials. 5µl aliquots of the supernatants were injected onto a reverse phase HPLC column (Scherzo C18 100 x 2.1mm, 1.7µ particle size and 100Å), equilibrated in solvent A (water/acetonitrile/formic acid, 100/3/0.1, all by vol) and eluted (200µL/min) with an increasing concentration of solvent B (45mM ammonium formate/acetonitrile, 65/35, vol/vol: min/%B; 0/0, 5/0, 30/32, 35/0, 45/0). The effluent from the column was directed to an electrospray ion source connected to a triple quadrupole mass

spectrometer (Agilent 6460) operating in the positive ion multiple reaction monitoring (MRM) mode. The intensities of peaks in selected MRM transitions were recorded at previously determined retention times and optimized instrumental settings (kynurenine m/z 209.0⇒192.0 at retention time (rt) 20.6 min; 2H5-kynurenine m/z 214.0⇒96.0 at rt 20.6 min; tryptophan m/z 205.0⇒188.0 at rt 22.4 min; 2H3-tryptophan 208.0⇒147.0 at rt 22.4 min).

The samples were divided into four batches (23 samples/batch), each sample was analyzed in duplicate, and each batch included ten standards (five dilutions, each in duplicate). The standards were prepared as above with pH 7.2 phosphate-buffered saline substituting for plasma, the same amount of internal standards, and increasing amounts of kynurenine (0, 50, 100, 200, and 400 pmol) and tryptophan (0, 1.25, 2.5, 5, and 10 nmol). The data from the standards was used to construct standard curves in which the ratio of peak intensities (ordinate; kynurenine/2H5-kynurenine or tryptophan/2H3-tryptophan/) was plotted against amount of kynurenine or tryptophan (abscissa); the kynurenine and tryptophan content of each sample was interpolated from the respective standard curves. The values for the duplicate samples were averaged. The limit of detection for kynurenine and tryptophan was around 50 fmol injected.

2.1.6 Humoral Immune Responses

Frozen serum samples drawn at baseline, week 5 and week 15 were shipped on dry ice to Seramatrix Corp. (Carlsbad, CA) and tested for antibody reactivity against 34 different putative tumor-antigens, namely CABYR, CSAG2, CTAG1B, CTAG2, CYCLINB1, CYCLIND1, GAGE1, HER2, HSPA4, HSPD1, HTERT, LDHC, MAGEA1, MAGEA3, MAGEB6, MICA, MUC1, MYCPB, NLRP4, P53, PBK, PRAME, SILV, SPANXA1, SSX2, SSX4, SSX5, SURVIVIN, TRIP4, TSSK6, TULP2, WT-1, XAGE and ZNF165. A positive score was returned for any measurement that was above 2x the 25th percentile of all antigens, patients and time points.

2.1.7 Statistics

A repeated measures analysis of variance was used to assess differences among patients for each serological marker at baseline and for each patient over time of treatment. Longitudinal immune responses for each patient were assessed in the context of survival data and summarized through quantile regression and compared as cohorts of the 2 treatment arms with the Mann Whitney test. Recursive partitioning analysis (Classification and Regression Tree, CART) allowed for the selection of those endpoints that could accurately classify patients into those who lived longer than the median survival versus those who did not (Salford Systems, CART software, San Diego, CA). Overall outcome was assessed through the log-rank test. Statistical significance was at the 5% level.

2.2 Results

2.2.1 Trial Design

As outlined above, 22 patients were consented and randomized into 2 treatment arms with 11 patients in each arm receiving either 1mg/kg or 10mg/kg of the TGFβ-neutralizing antibody, Fresolimumab. Not all patients completed the full course of treatment comprising 12 weeks of Fresolimumab injections concurrently with a couple of courses of 22.5Gy irradiation given to 2 metastatic sites and a final radiologic assessment and blood draw after 15 weeks (Figure 1A). Only 2 patients (18%) in the 1mg/kg arm and 7 patients (64%) in the 10mg/kg arm (Figure 1B) lasted to 15 weeks because of disease progression. A higher propensity to complete treatment in the 10mg/kg arm is also reflected in overall survival (median OS = 64.1 weeks versus 20 weeks at 1mg/kg, p=0.015 Log-rank test) (Figure 1C). 2 patients (N06 and N11) were still alive at last follow up after 207 and 129 weeks on study, respectively, and both patients were in the 10mg/kg arm. Although a detailed assessment of outcome data is not subject of this discussion here, all immunological responses were compared between treatment arms as well as assessed within the broader context of patient survival.

2.2.2 Basic blood composition (CBC data)

For the most part our patients had PBMC's counts that were well below the healthy volunteer cohort (Figure 2A, p=0.001) although still within normal range (0.8-3.2x10^6/ml). Interestingly, 7 of 9 patients in the 10mg/kg-arm responded to treatment with stable or rising PBMC counts whereas only 5 of 10 did in patients treated with 1mg/kg (Figure 2B, p=0.043).

2.2.3 Tumor-specific $CD8^+$ T cells

Of 22 patients entering this trial, 11 (50%) were HLA-A*0201 positive and therefore eligible for the tetramer and/or dextramer binding assay as were 6 of the 11 healthy controls (54.5%). One patient (N01) had a significant treatment delay of almost 9 months before starting again with the full course, which led to repeated blood draws at baseline and week 2. All in all there were 12 samples at baseline, 10 samples each at week 2 and week 5, and by the 15^{th} week there were 5 samples remaining. Minimum quality control requirements (see material and method section) were reached for all of these samples.

The threshold for positivity was based on healthy volunteers having a median and interquartile range (IQR) of survivin reactive $CD8^+$ T cells of 0.12 + 0.06% (Figure 3A). At baseline, excluding one who did not go past the 2 week time point, there were 3 patients (27%), namely N01, N03 and N05, all in the 1mg/kg GC1008 arm, who had pre-existing levels of survivin-reactive $CD8^+$ T cells above the threshold and in these increased further during treatment in a couple of cases. The third patient, N05, experienced a transient decline in survivin-specific $CD8^+$ T cells during the trial before returning to near pre-treatment levels by week 15. The majority of patients started with survivin-specific $CD8^+$ T cell levels within the normal, negative range and remained so throughout the course of treatment with the exception of patients N02, N014 and U03 who had above normal values at least at one point, either during or at the end of treatment (Figure 3A). Threshold aside, 64% (7 of 11) of patients responded with rising

survivin-reactive $CD8^+$ T cells early during treatment when compared to their individual baseline values (Figure 3B), but was rarely sustained. This may indicate that this approach, although moving in the right direction, was insufficient to sustain responses and overcome the regulatory networks.

A small number of patients (6) were tested for reactivity towards other, putative tumor antigens Muc-1, Her2/neu and Jarid1B. One patient was tested at all 4 time points, 3 patients at 3 time points, one patient with 2 time points and one patient with only a single time point totaling 5 baseline measurements, 5 at week 2, 4 at week 5 and a couple at 15 weeks. Remarkably, 4 of 5 patients (80%) had pre-existing T cell reactivity against JARID1B considering the healthy volunteer's values as the lower limit (0.11 + 0.02%, see above) (Figure 3C). The frequency of these cells appeared to fluctuate significantly during treatment but remained above the threshold for the most part. Only two patients (40%) had anti-Her2 T cell reactivity at baseline (N10 and U07, cut-off=0.17%), and both fell progressively during treatment (Table 1). Similarly, meaningful Muc1-specific T cell levels (cut-off = 0.17%) could be detected in two individuals before treatment (N10 and N14) but only one patient (N14) was able to respond with a transient Muc-1 T cell spike at week 2 (Table 1). In fact, patient N14 appeared to respond with a transient rise in tumor-specific T cells for all 4 tumor antigens (Table 1). Clearly, the number of patients in each treatment arm is not sufficient to allow us seeing trends in epitope spreading.

2.2.4 Memory subsets

Analysis of 10 of our patients for CD45RA and CCR7 expression revealed the classic T cell differentiation along the naïve-effector-memory axis, with relatively few effector cells in the CD4 compartment (Figure 4A) but many in the CD8 T cell subset (Figure 4C). Though beyond statistical significance, ranking according to survival suggested that the bigger the proportion of naïve CD4 at baseline the better the prognosis with a couple of exceptions (Figure 4A, p=n.s.). Similarly, in the 10mg/kg Fresolimumab treatment arm there was a positive association between survival and the ratio of CD8 effector memory to central memory cells at baseline that just failed to reach statistical significance (Figure 4E, r= 0.794, p=0.059).

Perhaps the most striking finding that the 10mg/kg Fresolimumab treatment group showed was an increase in the memory pool, especially of the central memory type. This came largely at the expense of effector CD8s and stood in stark contrast to the responses in the 1mg/kg arm where the memory pool began to diminish relative to a rising effector pool (Figure 4D) (1mg vs 10mg: CM, EM and Effector at week 0-2 p= 0.014-0.027, week 0-5 p=0.0021). This was echoed by similar tendencies in the CD4 compartment, although here there was less consistency (Figure 4B) (effector CD4 p=0.02; CM CD4 p=0.032).

2.2.5 Regulatory networks

Powerful regulatory networks exist to moderate immune responses and may in fact mirror immune activation, both in timing and magnitude. Enumeration of suppressor subsets is not restricted by HLA and therefore more samples (19 in total with 20

response patterns because of N01's treatment delay) were available for this type of analysis, which increased the statistical rigor. For T regulatory cells (Tregs), baseline levels for most patients were below those of our 11 healthy volunteers (median and IQR = 2.55 +/- 1.64% for patients versus 4.6 +/- 1.4% for controls; p value=0.000, Figure 5A). However, many showed an early rise 2 weeks after treatment initiation (p=0.005; Figure 5B). This was more common in the 10mg/kg-arm (6 of 7 - 86%) compared with 6 out of in the 1mg/kg arm (p=0.008 Figure 5B). This is also reflected in the extent of co-tracking between Tregs and survivin-reactive T cells which appeared more common in the higher antibody dose group (Figure 5C).

Suppressor cells of the myeloid compartment followed a pattern diametrically opposed to Tregs in that most of the patients (5 of 7; 71%) in the 10mg/kg group responded to treatment with declining monocytic myeloid-derived suppressor cells (mMDSCs) within 2 weeks whereas only 36% (4 of 11) of patients in the 1mg/kg group showed such an early decline (Tregs/mMDSC ratio, p=0.026 week 0-2 and p=0.036 week 0-5, Figure 6B and E). In other words, between 64-75% of all patients had Treg and mMDSC trends that contrasted one another, at least initially (Figure 6E). The early treatment-related decline in MDSCs was also true for the granulocytic subset (gMDSCs). In fact, this was true for most patients, regardless of the drug dose given (13 of 18, 72%, Figure 6D and E). The overall levels of gMDSCs varied widely at baseline around a median and IQR of 0.54 +/- 1.4% for all patients (Figure 6C) which was somewhat above what was seen in healthy volunteers (median and IQR = 0.36 +/- 0.21%, p value=0.53).

2.2.6 L-Tryptophan catabolism

Immune suppression through the activity of indoleamine 2,3-dioxygenase (IDO) or tryptophan 2,3-dioxygenase (TDO) results in a deficit in L-tryptophan and an excess in kynurenine that decreases T cell viability and function, and is commonly observed in cancer patients. The balance of plasma tryptophan and kynurenine can be a biomarker for disease activity and response to therapy but also a gage of general inflammatory status. Carefully collected plasma in highly-inert CTAD-tubes (BD Biosciences) followed by appropriate storage until liquid chromatographic/tandem mass spectrometric analysis allowed us to detect L-tryptophan and kynurenine at the expected micro-molar range of 20-98μM and 2-9μM, respectively, in our patients at baseline (Figure 7A). Unfortunately, samples were analyzed in two separate batches according to the study location (NYU versus UCLA) that varied significantly. Patients treated at UCLA tended to have higher L-tryptophan and lower kynurenine than NYU's patients resulting in lower Kynurenine-to-L-Tryptophan ratios at baseline (Figure 7A bottom). Reasons for this discrepancy are not entirely clear, but the majority of patients regardless of location and/or treatment arm responded with an early and progressive fall in plasma levels of L-tryptophan (Figure 7B top, p=0.004). Many, but not all, patients had a concomitant decline in kynurenine and those that did not were all treated at NYU (Figure 7B middle, p=0.025). Ultimately, it is the balance between these metabolites that determines the extent of immune suppression and the proportion of patients showing an encouraging shift of this balance in favor of L-tryptophan and presumably lessened suppression was higher in the 10mg group with 5 of 7 (71%) falling K/T ratio at week 2 versus 6 of 11 (55%) in the

1mg group though outside statistical significance (Figure 7B bottom). Of note, all of UCLA's patients presented with this favorable early shift towards rising L-tryptophan relatively to kynurenine, regardless of drug dose.

2.2.7 Humoral responses

We screened patient's sera for antibody responses against a panel of 34 common tumor antigens in an attempt to assess the involvement of the B cell compartment in our patient population (Table). Four patients had pre-existing responses to >5 of these antigens. Two of these patients, namely N09 and N03 significantly decreased their tumor-specific antibody load with time and both were in the 1mg/kg arm. Of the remaining 11 patients who started with low antibody reactivity, 3 increased in responsiveness to a score of >1 and all 3 had received 10mg/kg doses (U03, N11, and U05).

Of note, the 2 patients who converted to positive survivin-specific responses in the tetramer analysis (U03 and N02, Figure 3A) also had rising survivin antibody titers (not shown). Patient N03 had both, high pre-existing survivin-specific T cells (Figure 3A) and pre-existing survivin-reactive antibodies (not shown) but T cell and B cell responses against survivin were generally not correlative in these patients (not shown).

2.2.8 Summary of response patterns

The aim to find patterns of responses within complex, multi-dimensional immune monitoring data such as these can be rewarding and challenging in equal measures. In an attempt to dissect the impact of treatment on each endpoint and its correlation to outcome we used polar graphs and heat maps to provide a summary of those endpoints with the most striking and consistent response patterns (Figure 8). Polar graphs for instance give us a bird's eye view of the median relative change for each endpoint between 0-2 weeks (Figure 8A) and 0-5 weeks (Figure 8B). Clearly, Tregs ($p=0.004$), the ratio of Tregs to mMDSC ($p=0.026$), central memory CD8s ($p=0.027$), NK cells ($p=0.074$) and the yield of PBMCs ($p=0.051$) exhibit some of the biggest changes during treatment with 10mg/kg Fresolimumab that failed to materialize in the 1mg/kg-arm. The reverse is true for effector CD8s ($p=0.014$) and the ratio of kynurenine to tryptophan (n.s.), both selectively rise in the 1mg/kg arm only.

Finding clear patterns within a sum of individual responses is inherently more difficult but ranking patients according to survival and using the best survivor to rank the endpoints did in fact facilitate a meaningful heat map (Figure 8C). Three broad subsets of patients emerged. Patients who survived close to the median overall survival appeared to show very little global change (green). On either side fell patients who survived well above or below the median overall survival, and both presented with diametrically opposing changes over time. For one, immune endpoints that increased within 2 or 5 weeks (red) appear more common in the longest survivors whereas the worst-to-do patients predominantly show down-regulation of immune endpoints (blue). Secondly, those endpoints that do go up or down cluster differently in these 2 patient populations (top red -to-bottom blue versus top blue -to- bottom red).

Recursive partitioning analysis (Classification and Regression Tree, CART) was

performed on changes in response variables between baseline and week 2 and 5 to elucidate predictability of a patient's outcome below/above median survival. CART analysis allowed accurate survival classification based on 2-week changes in CD8/mMDSC ratios (82.4% overall correct). Whereas 5-week changes in Tregs and the ration of CD8/Treg together had a total overall correct classification of 93.75%.

2.3 Discussion

Many tumors make large amounts of TGFβ that is highly immunosuppressive and effective blocking of TGFβ is challenging precisely because of the high levels and its ubiquity. Targeting specific functions of TGFβ is even more difficult due to the diverse roles this cytokine plays. For instance, knockout studies have shown that intercepting the TGFβ network can have enormous consequences ranging from excessive inflammation with suboptimal M2 macrophage polarization to loss of peripheral tolerance, even lethality (10, 11). CD8+ T cells that are genetically rendered insensitive to TGFβ showed a lot of promise as they became more able to mediate tumor regression (12). However, knockout mouse models are very different from intermittent interruption of signaling using an antibody in adult humans as was done here, but preclinical studies with this approach clearly demonstrated that TGFβ inhibits the ability of radiation therapy to generate an in situ tumor vaccine and abscopal effects at distant tumor sites (13), giving some rationale for this attempt to examine this concept in metastatic breast cancer the clinic.

The number of patients in this study was small, and the cancers were advanced, so caution should be exercised in the interpretation of the limited data. One potential variable is the intrinsic response of individual tumors to TGFβ. This is dependent of mutations within the TGFβ signaling pathways, and also ER status. Some ER+ tumors appear to maintain the TGFβ-driven tumor suppression axis for a long time (14) and blocking TGFβ under such circumstances might have a detrimental element. In our study, estrogen receptor signaling did not appear to have played a significant role as the six longest survivors in the 10mg/kg group were all ER+. In general, our patients were heterogenous in terms of ER expression with 11 patients (65%) ER+ and 6 (35%) ER-. In spite of these and other caveats, several interesting findings came from examination of the immune responses to treatment that might guide future investigations.

Surprisingly, patients in the 10mg/kg arm responded to TGFβ blockade with an early, almost uniform rise in circulating Tregs. This may seem counterintuitive because TGFβ is known to be produced by one Treg subset and to support the survival and maintenance of Tregs, but it does so while also inhibiting their proliferation. The increases in Tregs are therefore perhaps not so surprising. The Treg levels appeared in fact to be oscillating in our patients, which may have been due to the concomitant loss in survival cues necessary to maintain levels or to intermittent recovery in TGFβ. More importantly, whether such Treg spikes relate to inadequate anti-tumor T cell immunity and poor outcomes, as one would expect in breast cancer, remains to be determined (15, 16). It certainly did not appear to be of disadvantage to our patients.

Our results also suggest that TGFβ blockade may have interrupted the IDO-Treg-MDSC axis that tends to move in unison when driving systemic immune suppression (17). Even though circulating levels of tryptophan fell and Tregs rose in most of our

patients suggestive of heightened IDO activity, this appeared to be uncoupled from the shrinking MDSC pool, especially in the 10mg/kg arm. That there is a cross-talk between Tregs and MDSCs has been suggested by others (18) but how much of this depends on TGFβ is unclear. Certainly, TGFβ drives an extensive regulatory network that strictly controls central T cell development and tolerance as well as T cell homeostasis and differentiation in the periphery (19).

Perhaps one of the most intriguing findings of this study pertains to T cell homeostasis and differentiation and the fact that the higher dose of anti-TGFβ antibody clearly boosted the CD8 memory pool, especially the central memory type, to the detriment of T effector cells. Similar findings have been reported in preclinical tumor models where genetic targeting of TGFβ signaling promoted memory T cell development locally as well as systemically (20). The notion that TGFβ puts a limit on central memory development in human blood is not new and clearly speaks to the crucial role this pleiotropic cytokine plays in T cell homeostasis (21), but it is interesting that this can be seen in humans undergoing TGFβ blockade. It is of interest also because T cell inflammation of the memory type correlates with better prognosis in colorectal cancer presumably through stronger recall responses (22, 23). In fact, it seems that CD8 memory T cells infiltration into the tumor site might be part of what is needed to turn an immunotherapy patient into a responder (24).

It is tempting to ascribe the difference in survival between the 10mg/kg arm and the 1mg/kg to the immune effects in supporting a memory CD8 T cell response and decreased MDSCs but in reality the small patient numbers and the relatively short survival times overall make this debatable. Also, in spite of the altered immunity, it is also clear that the strategy of blocking TGFβ alone is unlikely to be sufficient in controlling tumor growth in most patients even when combined with radiation (25) and that this approach is likely to be only one element in a cohesive immunotherapy strategy to be employed with radiation therapy.

2.4 REFERENCES

1. Bouquet F, Pal A, Pilones KA, Demaria S, Hann B, Akhurst RJ, et al. TGFbeta1 inhibition increases the radiosensitivity of breast cancer cells in vitro and promotes tumor control by radiation in vivo. Clin Cancer Res. 2011;17(21):6754-65.
2. Miller LD, Chou JA, Black MA, Print C, Chifman J, Alistar A, et al. Immunogenic Subtypes of Breast Cancer Delineated by Gene Classifiers of Immune Responsiveness. Cancer immunology research. 2016;4(7):600-10.
3. Andersen MH, Pedersen LO, Capeller B, Brocker EB, Becker JC, thor Straten P. Spontaneous cytotoxic T-cell responses against survivin-derived MHC class I-restricted T-cell epitopes in situ as well as ex vivo in cancer patients. Cancer Res. 2001;61(16):5964-8.
4. Schaue D, Comin-Anduix B, Ribas A, Zhang L, Goodglick L, Sayre JW, et al. T-cell responses to survivin in cancer patients undergoing radiation therapy. Clin Cancer Res. 2008;14(15):4883-90.
5. Coleman JA, Correa I, Cooper L, Bohnenkamp HR, Poulsom R, Burchell JM, et al. T cells reactive with HLA-A*0201 peptides from the histone demethylase JARID1B are found in the circulation of breast cancer patients. Int J Cancer. 2011;128(9):2114-24.
6. Guckel B, Rentzsch C, Nastke MD, Marme A, Gruber I, Stevanovic S, et al. Pre-existing T-cell immunity against mucin-1 in breast cancer patients and healthy volunteers. J Cancer Res Clin Oncol. 2006;132(4):265-74.

7. Domschke C, Schuetz F, Ge Y, Seibel T, Falk C, Brors B, et al. Intratumoral cytokines and tumor cell biology determine spontaneous breast cancer-specific immune responses and their correlation to prognosis. Cancer Res. 2009;69(21):8420-8.
8. Comin-Anduix B, Gualberto A, Glaspy JA, Seja E, Ontiveros M, Reardon DL, et al. Definition of an immunologic response using the major histocompatibility complex tetramer and enzyme-linked immunospot assays. Clin Cancer Res. 2006;12(1):107-16.
9. Midttun O, Hustad S, Ueland PM. Quantitative profiling of biomarkers related to B-vitamin status, tryptophan metabolism and inflammation in human plasma by liquid chromatography/tandem mass spectrometry. Rapid communications in mass spectrometry : RCM. 2009;23(9):1371-9.
10. Gong D, Shi W, Yi SJ, Chen H, Groffen J, Heisterkamp N. TGFbeta signaling plays a critical role in promoting alternative macrophage activation. BMC immunology. 2012;13:31.
11. Kulkarni AB, Huh CG, Becker D, Geiser A, Lyght M, Flanders KC, et al. Transforming growth factor beta 1 null mutation in mice causes excessive inflammatory response and early death. Proc Natl Acad Sci U S A. 1993;90(2):770-4.
12. Quatromoni JG, Wang Y, Vo DD, Morris LF, Jazirehi AR, McBride W, et al. T cell receptor (TCR)-transgenic CD8 lymphocytes rendered insensitive to transforming growth factor beta (TGFbeta) signaling mediate superior tumor regression in an animal model of adoptive cell therapy. J Transl Med. 2012;10:127.
13. Vanpouille-Box C, Diamond JM, Pilones KA, Zavadil J, Babb JS, Formenti SC, et al. TGFbeta Is a Master Regulator of Radiation Therapy-Induced Antitumor Immunity. Cancer Res. 2015;75(11):2232-42.
14. Sato M, Kadota M, Tang B, Yang HH, Yang YA, Shan M, et al. An integrated genomic approach identifies persistent tumor suppressive effects of transforming growth factor-beta in human breast cancer. Breast cancer research : BCR. 2014;16(3):R57.
15. Verma C, Eremin JM, Robins A, Bennett AJ, Cowley GP, El-Sheemy MA, et al. Abnormal T regulatory cells (Tregs: FOXP3+, CTLA-4+), myeloid-derived suppressor cells (MDSCs: monocytic, granulocytic) and polarised T helper cell profiles (Th1, Th2, Th17) in women with large and locally advanced breast cancers undergoing neoadjuvant chemotherapy (NAC) and surgery: failure of abolition of abnormal treg profile with treatment and correlation of treg levels with pathological response to NAC. J Transl Med. 2013;11:16.
16. Bailur JK, Gueckel B, Derhovanessian E, Pawelec G. Presence of circulating Her2-reactive CD8 + T-cells is associated with lower frequencies of myeloid-derived suppressor cells and regulatory T cells, and better survival in older breast cancer patients. Breast cancer research : BCR. 2015;17:34.
17. Holmgaard RB, Zamarin D, Li Y, Gasmi B, Munn DH, Allison JP, et al. Tumor-Expressed IDO Recruits and Activates MDSCs in a Treg-Dependent Manner. Cell reports. 2015;13(2):412-24.
18. Fujimura T, Kambayashi Y, Aiba S. Crosstalk between regulatory T cells (Tregs) and myeloid derived suppressor cells (MDSCs) during melanoma growth. Oncoimmunology. 2012;1(8):1433-4.
19. Li MO, Flavell RA. TGF-beta: a master of all T cell trades. Cell. 2008;134(3):392-404.
20. Gate D, Danielpour M, Rodriguez J, Jr., Kim GB, Levy R, Bannykh S, et al. T-cell TGF-beta signaling abrogation restricts medulloblastoma progression. Proc Natl Acad Sci U S A. 2014;111(33):E3458-66.
21. Takai S, Schlom J, Tucker J, Tsang KY, Greiner JW. Inhibition of TGF-beta1 signaling promotes central memory T cell differentiation. J Immunol. 2013;191(5):2299-307.
22. Pages F, Berger A, Camus M, Sanchez-Cabo F, Costes A, Molidor R, et al. Effector memory T cells, early metastasis, and survival in colorectal cancer. N Engl J Med. 2005;353(25):2654-66.
23. Koelzer VH, Lugli A, Dawson H, Hadrich M, Berger MD, Borner M, et al. CD8/CD45RO T-cell infiltration in endoscopic biopsies of colorectal cancer predicts nodal metastasis and survival. J Transl Med. 2014;12:81.
24. Ribas A, Shin DS, Zaretsky J, Frederiksen J, Cornish A, Avramis E, et al. PD-1 Blockade Expands Intratumoral Memory T Cells. Cancer immunology research. 2016;4(3):194-203.
25. Jackson CM, Kochel CM, Nirschl CJ, Durham NM, Ruzevick J, Alme A, et al. Systemic Tolerance Mediated by Melanoma Brain Tumors Is Reversible by Radiotherapy and Vaccination. Clin Cancer Res. 2016;22(5):1161-72.

2.5 Figures

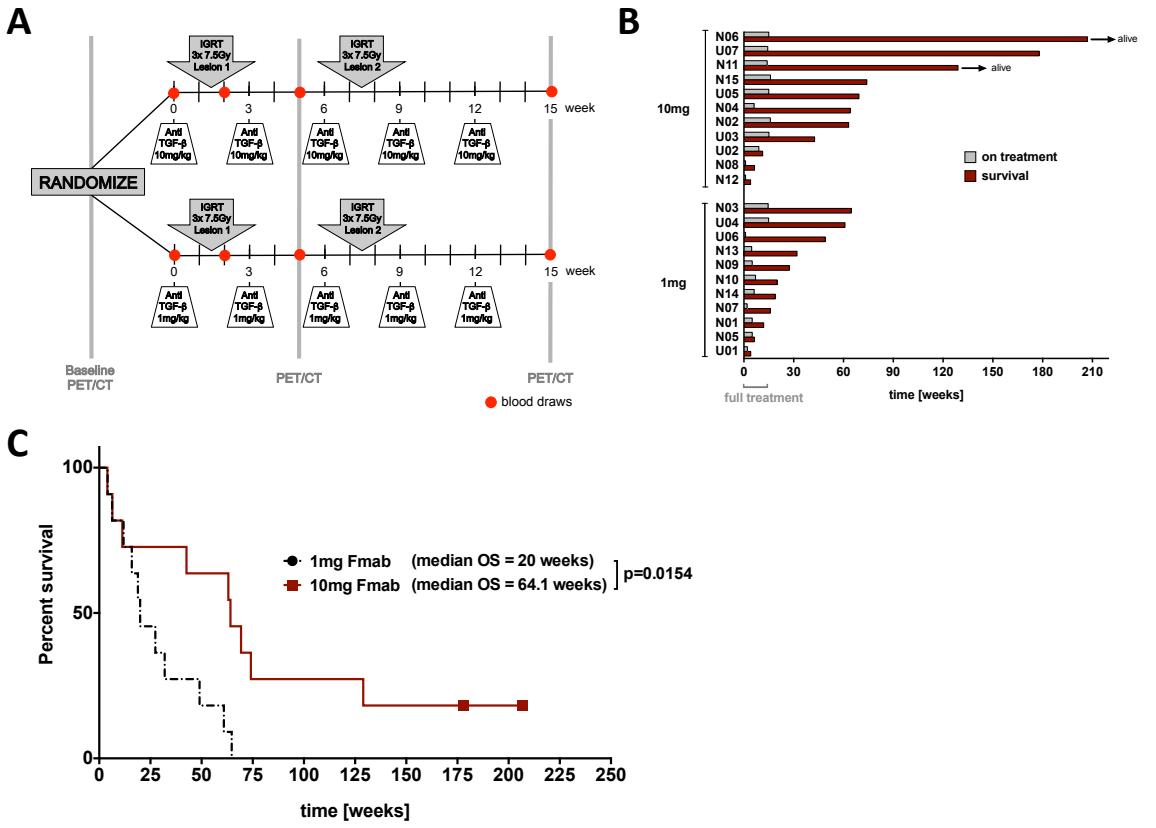

FIGURE 1: Trial design and outcome in 22 metastatic breast cancer patients treated with Fesolimumab and Radiation (#NCT01401062). **A)** Patients received either 1mg/kg or 10mg/kg i.v. of Fresolimumab every three weeks in week 0, 3, 6, 9 and 12 for a total of 5 cycles. External beam radiation of 3x 7.5Gy was given to one metastatic site in week 1 and repeated to a second metastatic site in week 7. Blood was drawn for immune monitoring purposes (red dots) at baseline, after the first cycle of antibody infusion and radiation (week 2), after the second cylce of antibody infusion (week 5) and after completion of treatment (week 15). Serial PET/CT imaging allowed for tumor growth assessment. **B)** Patients in the higher dose arm were more likely to complete the 15-week treatment (gray bars) and to live longer (red bars). **C)** Kaplan Meyer plot showing a relative overall survival benefit in the 10mg-arm of 44 weeks (red line) (median overall survival 64 weeks versus 20 weeks, log-rank test p=0.015). (N=treated at NYU; U=treated at UCLA).

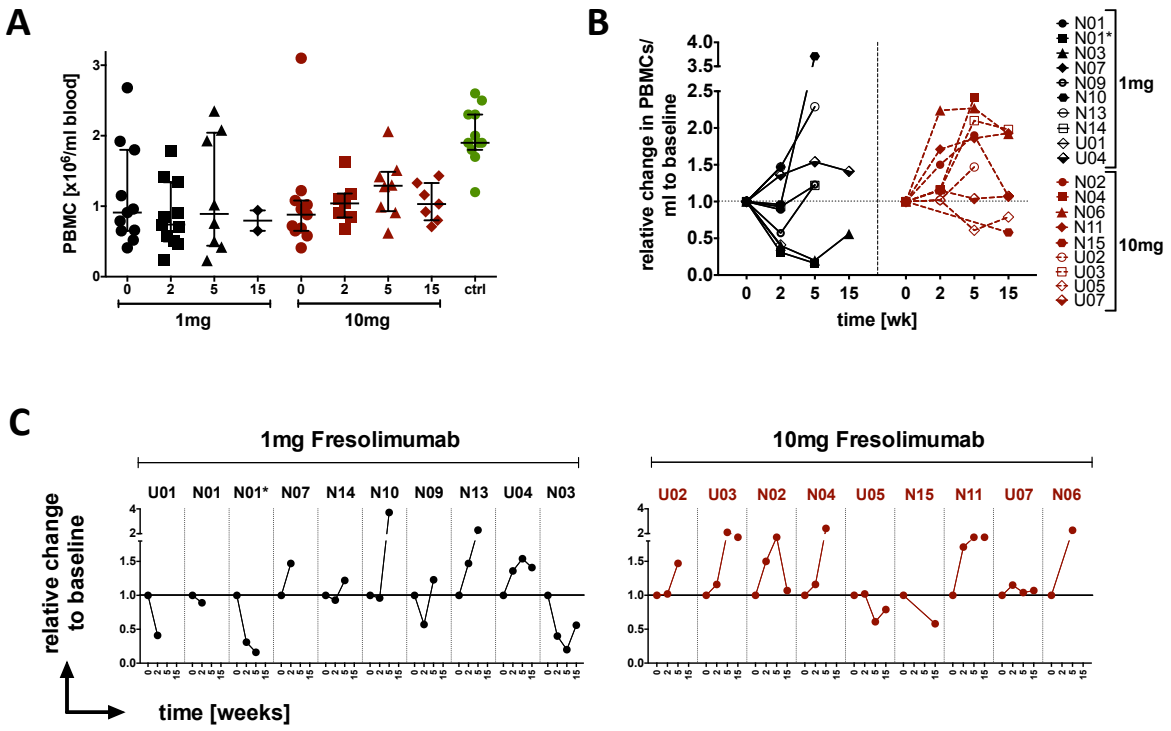

FIGURE 2: High-dose TGFβ inhibition prevents radiation-induced white cell nadirs. PBMCs levels isolated from blood samples over Ficoll gradient rose temporarily in patients receiving 10mg Fresolimumab (red) according to **A)** absolute levels; **B)** grouped individual changes relative to each individual's baseline value or **C)** individual changes ranked according to survival from shortest (left) to longest (right). (N=treated at NYU; U=treated at UCLA; black=1mg and red=10mg Fresolimumab, green=11 healthy volunteers)

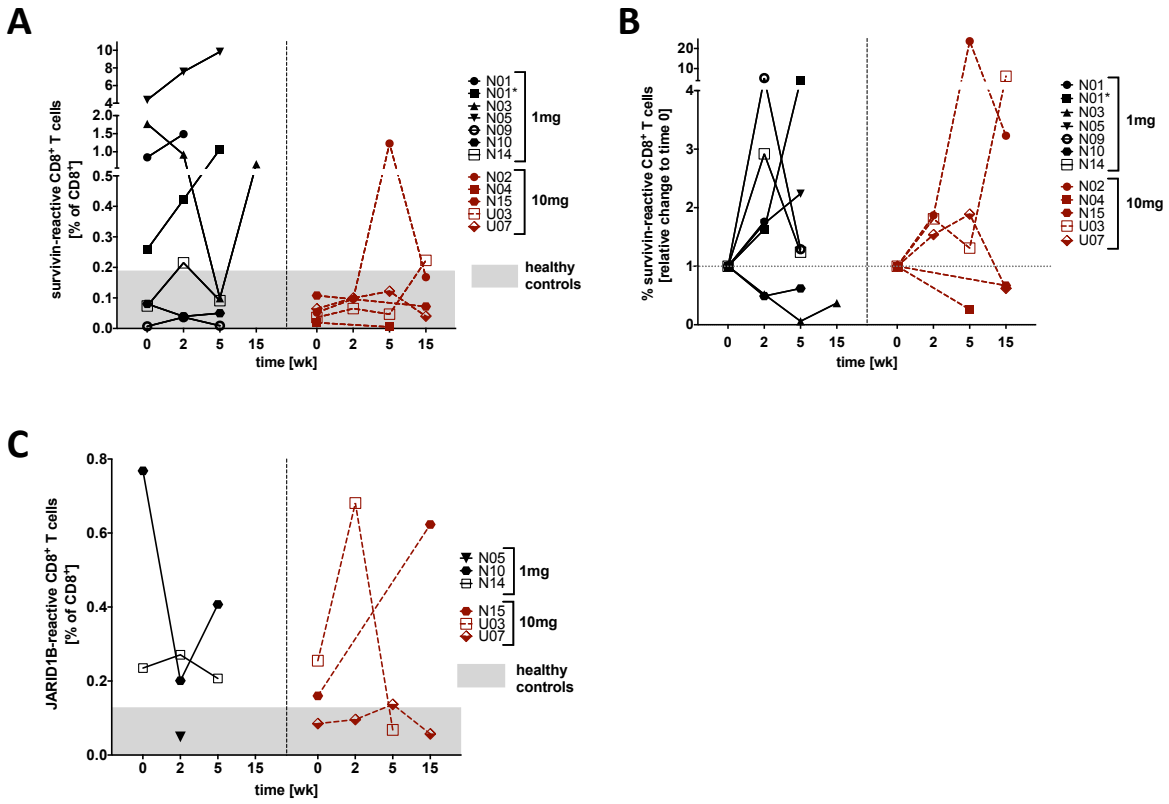

FIGURE 3: Levels of circulating survivin-reactive $CD8^+$ T cells increase in some patients during treatment with Fesolimumab and Radiation. Tetramer/dextramer staining data are shown as **A)** % survivin-positive $CD8^+$ T cells over the course of a 15 week treatment or **B)** as relative change to baseline for each individual patient. **C)** Level of circulating JARID1B-reactive $CD8^+$ T cells. (N=NYU patient; U=UCLA patient; black=1mg and red=10mg Fresolimumab). The presumed threshold of median + IQR of n=6 healthy control levels (0.18%) is indicated in gray.

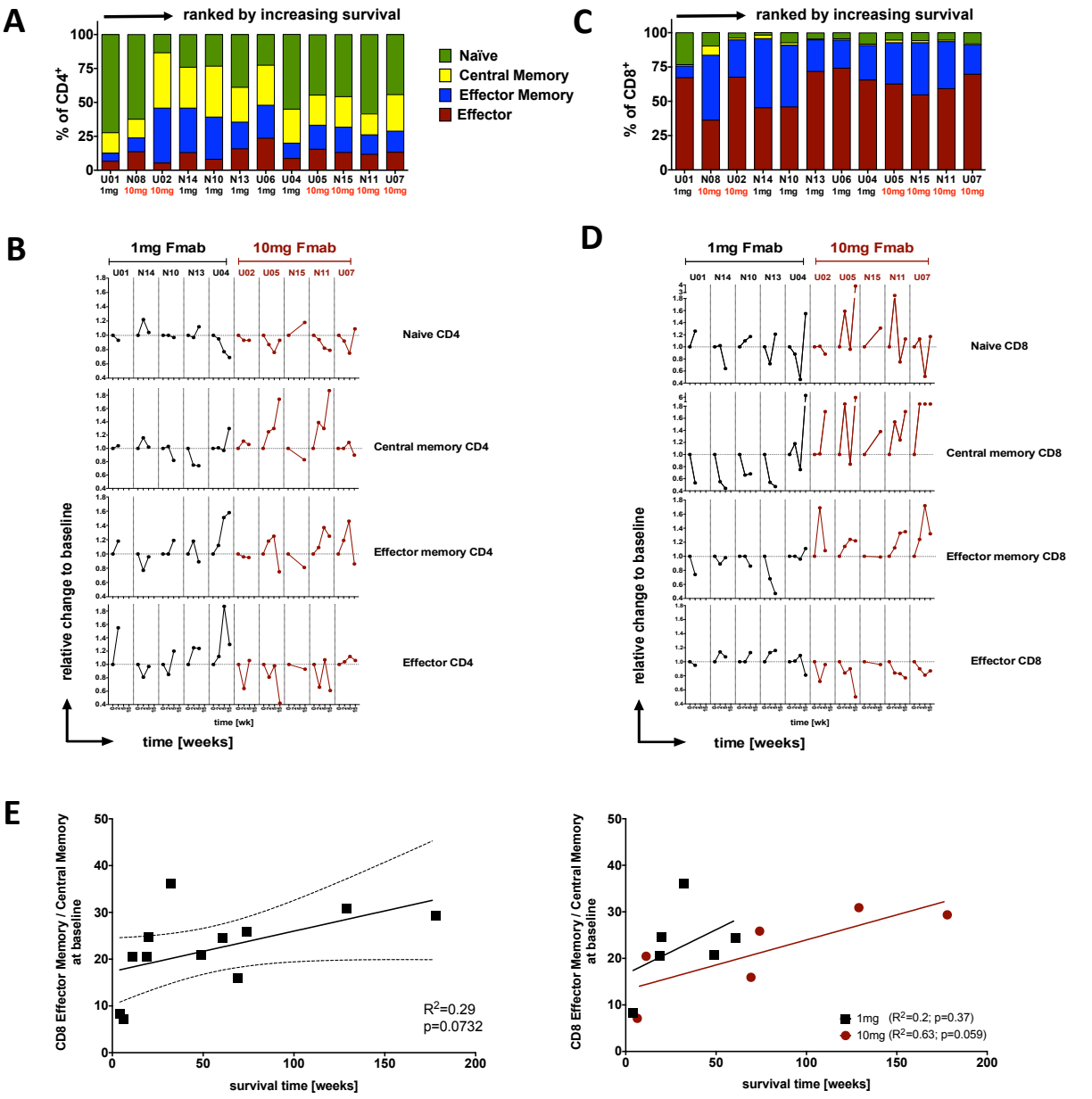

FIGURE 4: Breast cancer patients responded to 10mg Fesolimumab and Radiation with rising memory CD8+ T cells in their circulation. T cell differentiation was assessed according to CCR7 and CD45RA expression within each CD4+ or CD8+ T cell pool giving naïve T cells (CCR7+CD45RA+), Central memory (CCR7+CD45RA-), Effector memory (CCR7-CD45RA-) and Effector cells (CCR7-CD45RA+). Data are shown as individual baseline values ranked according to survival in **A)** the CD4+ compartment or **C)** the CD8+ compartment or as individual changes over time in **B)** and **D)**, respectively. **E)** Pre-treatment effector memory to central memory CD8+ T cell ratios positively correlated with outcome in the 10mg-arm (p=0.059).

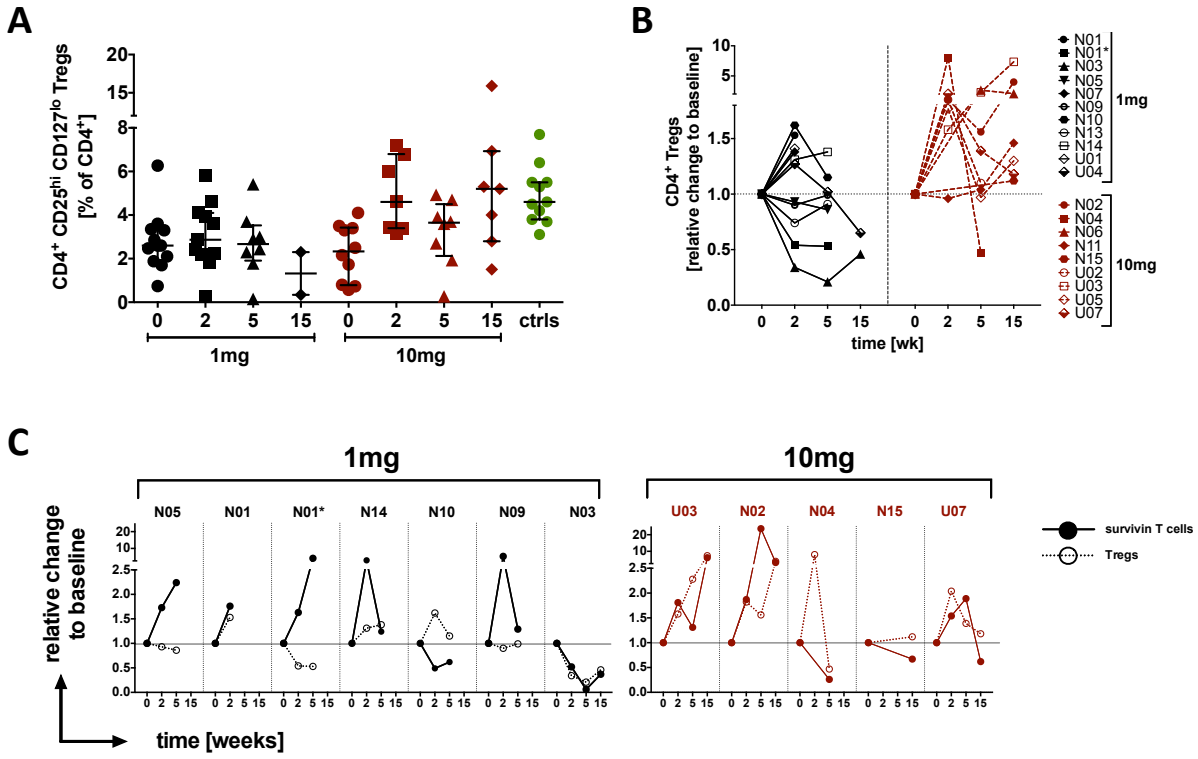

FIGURE 5: Breast cancer patients have relatively fewer circulating $T_{regulatory}$ cells than healthy volunteers but respond to high-dose TGFβ blockade plus Radiation with an oscillating rise. Data are % of CD4 cells that highly express CD25 while being low or negative for CD127 as **A)** individual points or **B)** as relative change over time to individual's baseline values. **C)** Individual changes in CD4+ Tregs side-by-side survivin-reactive CD8+ T cells changes. Patients were ranked according to increasing survival within each treatment arm. (N=treated at NYU; U=treated at UCLA; black=1mg and red=10mg Fresolimumab, green=11 healthy volunteers)

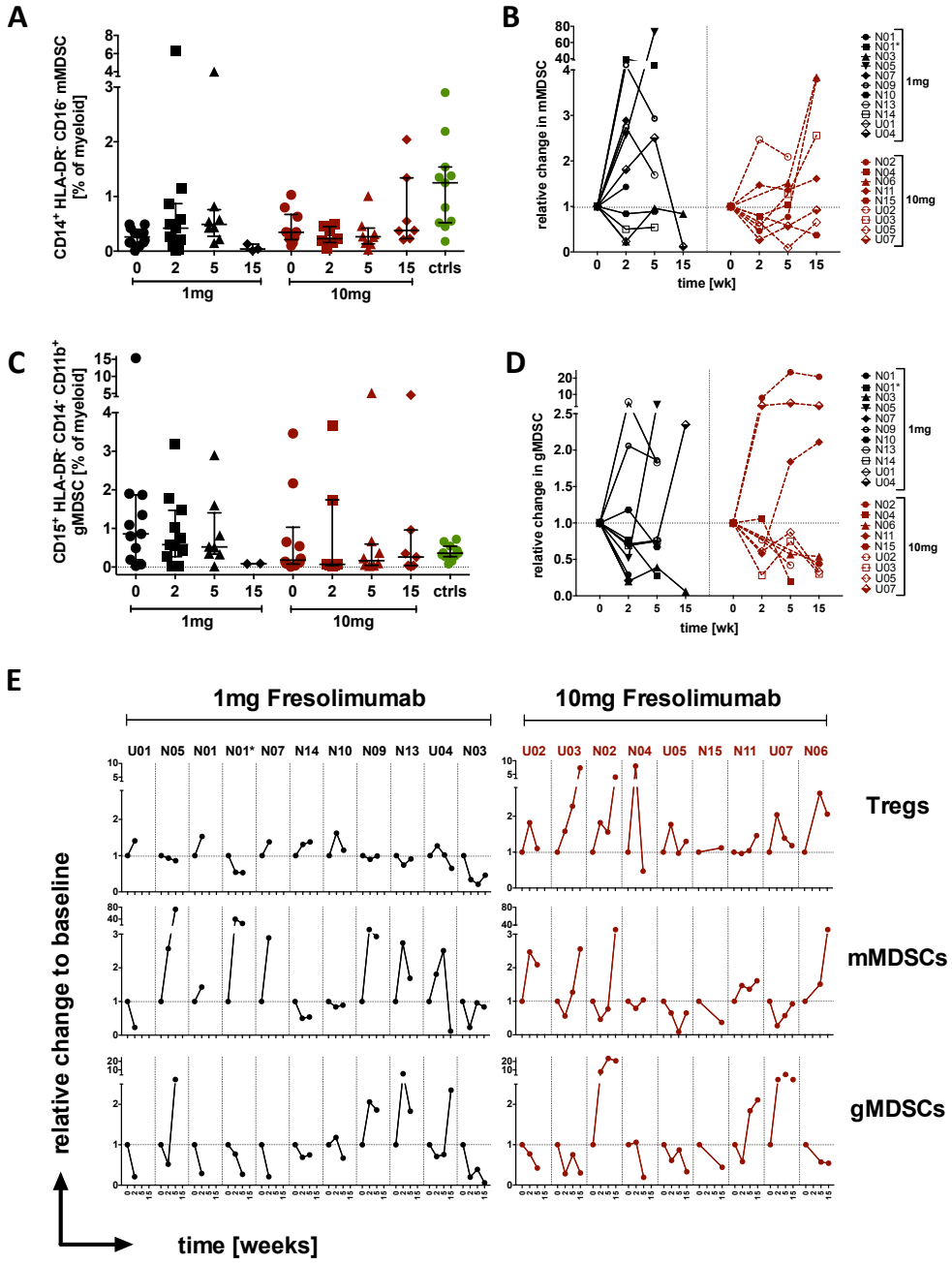

FIGURE 6: High-dose TGFβ blockade combined with radiation reduce regulatory networks within the myeloid compartment. Myeloid cells with the monocytic (CD14+DR-CD16-) or the granulocytic (CD15+DR-CD14-CD11b+) myeloid-derived suppressor cell profile are shown as individual points **A)** and **C)** or as relative change over time to individual's baseline values **B)** and **D)**. **E)** Changes in myeloid suppression is often diametrically opposed to those in Treg (top). Patients were ranked according to survival from shortest (left) to longest (right) within each treatment arm. (N=treated at NYU; U=treated at UCLA; black=1mg and red=10mg Fresolimumab, green=11 healthy volunteers)

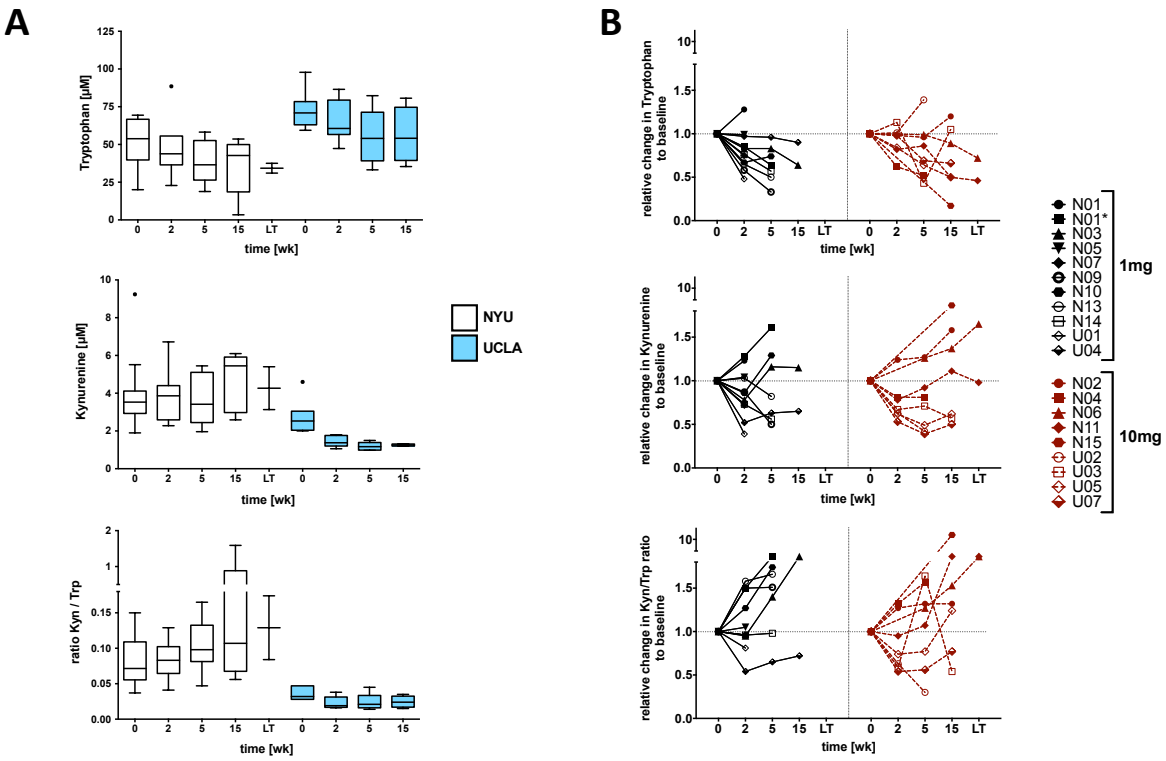

FIGURE 7: Fresolimumab and radiation can provide a favorable shift in Tryptophan metabolism towards L-Tryptophan and away from Kynurenine in some patients. Patient's plasma samples were analyzed in two batches according to treatment location (NYU vs UCLA) by liquid chromatographic/tandem mass spectrometry. Data are **A)** median and IQR (Tukey graph; whiskers 1.5xIQR) for each batch (NYU=white, UCLA=blue) or **B)** relative changes for each patient over time (N=treated at NYU; U=treated at UCLA; black=1mg and red=10mg Fresolimumab).

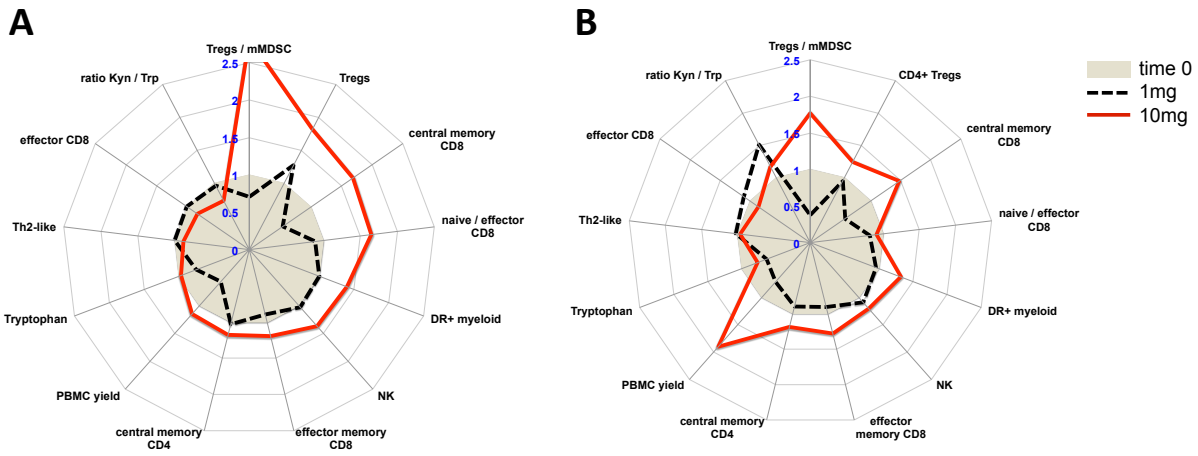

C

shortest survival → longest survival

treatment week	endpoint	survival below median									survival above median								
2	mMDSC	0.23	2.57	2.47	39.64	2.89	0.50	0.84	5.78	2.74	0.56	1.81	0.46	0.79	0.23	0.65	1.47	0.27
	myeloid cells	1.50	1.11	1.24	1.05	1.59	0.94	1.21	0.73	1.20	1.02	1.81	0.81	1.08	1.25	1.63	1.35	0.43
	CD8 / gMDSC	4.08	1.84	0.53	0.72	3.56	1.47	0.70	0.32	0.19	4.21	1.26	0.12	0.93	3.02	0.80	1.71	0.46
	Tryptophan / Tregs	0.3	1.1	0.6	1.6	0.5	0.6	0.4	0.6	0.9	0.7	0.8	0.5	0.1	2.4	0.5	0.9	0.5
	Kynurenine	0.39	1.04	0.63	1.28	0.72	0.73	0.86	0.87	1.03	0.67	0.52	1.24	0.81	0.78	0.62	0.78	0.53
	ratio K:T	0.81	1.05	0.63	1.50	0.96	0.96	1.27	1.50	1.58	0.59	0.54	1.27	1.32	0.95	0.74	0.95	0.54
	CD8 / Tregs	0.61	1.04	0.22	1.03	0.54	0.8	0.53	0.72	1.37	0.74	0.70	0.5	0.1	1.8	0.28	1.03	0.70
	Th2-like	1.01	0.97	1.10	2.00	0.84	1.08	1.15	0.97	1.14	0.88	1.00	1.14	0.69	1.22	0.83	0.92	0.86
	Tryptophan	0.48	0.99	1.01	0.85	0.75	0.76	0.67	0.58	0.65	1.13	0.97	0.98	0.62	0.83	0.84	0.82	0.98
	NK cells	1.87	1.03	1.37	0.77	3.20	0.86	1.46	0.19	0.84	1.67	1.45	1.36	1.48	0.83	1.38	1.07	1.07
	CD4/8 ratio	0.98	1.45	1.18	5.04	1.10	1.19	1.00	1.14	1.01	0.71	0.84	1.16	0.57	6.44	1.17	0.89	1.12
	PBMC yield	0.41		1.02	0.31	1.47	0.93	0.96	0.57	1.47	1.16	1.36	1.50	1.16	0.40	1.02	1.71	1.15
	mDCs	2.80	1.02	0.31	0.34	0.32	1.31	1.51	0.91	0.57	1.04	0.65	0.75	2.88	2.19	2.66	0.48	1.34
	CD8	0.86	0.96	0.41	0.55	0.74	1.02	0.82	0.65	1.01	1.16	0.89	0.98	0.98	0.60	0.49	0.99	1.43
	non class monocytes	2.84	0.73	4.27	1.47	1.22	1.33	1.02	0.40	0.82	1.00	1.43	0.55	1.81	1.63	4.08	1.64	1.48
	Th1-like	0.74	2.33	1.28	1.58	3.18	0.75	0.54	0.89	1.03	1.32	0.94	0.73	74.54	0.92	2.08	1.23	1.50
	CD4	0.84	1.39	0.48	2.76	0.81	1.21	0.82	0.74	1.02	0.82	0.75	1.14	0.56	3.85	0.57	0.88	1.60
	classical / non-class monocytes	0.22	3.08	0.38	0.75	0.70	0.74	0.68	2.99	1.34	0.94	0.68	1.43	0.87	0.67	0.19	1.97	1.88
	Th17-like	2.98	0.75	0.40	0.21	1.43	0.93	0.46	0.93	0.16	1.17	1.12	0.99	0.96	0.37	2.45	1.19	1.89
	Tregs	1.41	0.93	1.82	0.54	1.38	1.31	1.62	0.90	0.74	1.58	1.27	1.82	8.06	0.34	1.77	0.96	2.04
	classical monocytes	0.61	2.26	1.62	1.10	0.86	0.99	0.69	1.18	1.11	0.93	0.97	0.79	1.56	1.10	0.76	3.23	2.78
	gMDSC	0.21	0.52	0.77	0.77	0.21	0.69	1.18	2.06	5.37	0.28	0.71	7.92	1.06	0.20	0.61	0.58	3.13
	CD8 / myeloid	0.57	0.86	0.33	0.53	0.47	1.08	0.68	0.90	0.84	1.14	0.49	1.22	0.91	0.48	0.30	0.73	3.32
	CD4 / myeloid	0.56	1.24	0.39	2.64	0.51	1.28	0.68	1.03	0.85	0.80	0.41	1.41	0.52	3.09	0.35	0.65	3.72
	CD8 / mMDSC	3.74	0.38	0.17	0.01	0.26	2.04	0.98	0.13	0.37	2.08	0.49	2.15	1.24	2.66	0.75	0.67	5.34
	Tregs / mMDSC	6.15	0.36	0.74	0.01	0.48	2.63	1.93	0.16	0.27	2.82	0.70	3.97	10.18	1.51	2.72	0.65	7.60

treatment week	endpoint	survival below median							survival above median							
5	mMDSC	72.94	2.09	25.21	0.54	0.89	2.93	1.69	1.27	2.51	0.77	1.04	0.96	0.09	1.36	0.57	1.51
	myeloid cells	2.63	1.16	1.17	0.82	1.37	0.84	1.31	1.34	1.41	0.78	1.27	2.09	1.22	1.10	0.53	1.10
	CD8 / gMDSC	0.13	1.73	1.32	1.58	0.89	0.36	0.51	1.18	1.64	0.05	5.10	2.36	1.02	0.64	0.34	0.91
	Tryptophan / Tregs		1.3	1.2	0.4	0.6	0.3	0.5	0.2	0.9	0.6	1.1	4.0	0.7	0.8	0.5	0.4
	Kynurenine		0.42	1.61	0.56	1.29	0.50	0.82	0.71	0.63	1.27	0.81	1.16	0.49	0.92	0.39	1.26
	ratio K:T		0.30	2.53	0.98	1.74	1.51	1.66	1.64	0.65	1.32	1.57	1.40	0.77	1.07	0.56	1.27
	CD8 / Tregs	0.56	0.66	0.67	0.9	0.52	0.67	1.03	0.39	1.21	0.7	2.1	4.4	0.92	1.13	1.14	0.2
	Th2-like	1.01	0.97	1.93	1.05	1.04	0.81	1.15	0.97	1.01	1.71	0.99	1.01	0.84	0.91	0.81	1.02
	Tryptophan		1.39	0.64	0.57	0.74	0.33	0.50	0.43	0.96	0.96	0.52	0.83	0.64	0.86	0.69	0.99
	NK cells	0.36	2.09	2.74	1.13	1.16	1.05	0.93	1.52	1.53	0.98	1.13	0.97	1.43	1.29	0.58	0.41
	CD4/8 ratio	0.68	0.65	5.30	0.88	1.02	1.12	1.02	0.71	0.68	0.84	1.19	1.30	1.19	0.70	0.91	2.18
	PBMC yield	1.47	0.16	1.22	3.71	1.23	2.29	2.10	1.54	1.90	2.42	0.20	0.61		1.86	1.04	2.27
	mDCs	2.26	0.14	0.20	1.64	0.89	0.88	0.62	1.24	0.97	0.65	1.36	1.36	10.46	0.69	1.00	0.27
	CD8	0.49	0.73	0.35	1.18	0.60	0.66	0.93	0.88	1.24	1.12	0.98	0.92	0.89	1.17	1.58	0.52
	non class monocytes	0.24	2.25	1.69	1.62	0.67	1.51	1.06	0.98	0.52	0.46	0.55	0.65	3.94	1.90	0.59	0.35
	Th1-like	0.38	2.15	3.79	0.74	0.79	1.44	0.95	1.14	0.84	0.01	4.76	1.67	1.75	1.29	1.42	6.66
	CD4	0.33	0.48	1.85	1.04	0.61	0.74	0.96	0.62	0.85	0.94	1.17	1.19	1.06	0.82	1.44	1.14
	classical / non-classical monocytes	3.62	0.58	0.40	0.58	1.28	1.10	1.12	0.92	1.60	1.95	1.20	1.62	0.21	1.53	3.81	2.20
	Th17-like	1.52	0.48	0.17	2.07	0.99	1.01	0.21	1.05	1.18	0.31	0.96	0.93	3.10	1.01	3.00	0.24
	Tregs	0.86	1.10	0.53	1.38	1.15	0.99	0.91	2.28	1.02	1.56	0.47	0.21	0.97	1.04	1.39	2.64
	classical monocytes	0.87	1.30	0.67	0.93	0.86	1.67	1.19	0.90	0.84	0.89	0.66	1.06	0.82	2.91	2.25	0.78
	gMDSC	3.62	0.42	0.27	0.75	0.67	1.86	1.83	0.75	0.76	23.65	0.19	0.39	0.87	1.84	4.66	0.57
	CD8 / myeloid	0.19	0.63	0.30	1.44	0.44	0.79	0.71	0.66	0.88	1.43	0.78	0.44	0.73	1.07	2.98	0.48
	CD4 / myeloid	0.13	0.41	1.58	1.27	0.44	0.88	0.73	0.47	0.60	1.20	0.92	0.57	0.87	0.75	2.71	1.04
	CD8 / mMDSC	0.01	0.35	0.01	2.19	0.67	0.23	0.55	0.70	0.50	1.45	0.94	0.96	10.16	0.86	2.75	0.34
	Tregs / mMDSC	0.01	0.53	0.02	2.55	1.28	0.34	0.54	1.80	0.41	2.02	0.45	0.22	11.06	0.76	2.42	1.74

FIGURE 8: Systemic TGFβ blockade and local hypofractionated radiation evoke immunological response patterns that correlate with outcome. Polar graphs illustrate median relative changes during **A)** week 0-2 and **B)** week 0 to 5 for those endpoints that were different between treatment arms (gay circle = 1 (baseline), >1 increase; <1 decrease, solid red line =10mg Fresolimumab; dotted black line = 1mg Fresolimumab). **C)** Patients are ranked according to survival with their individual immunological responses during 2 weeks and 5 weeks heat mapped. (blue=decrease; red=increase; green=no change).

Table 1: Levels of circulating tumor-specific CD8+ T cells with reactivity for JARID1B, Muc1 or Her2 in breast cancer patients with HLA-A*0201 status. Cells were stained with dextramers presenting the JARID1B peptide (QLYALPCVL), Mucin-1 (STAPPVHNV) and Her2/neu (KIFGSLAFL) and co-stained for $CD8^+$. Non-viable cells were excluded on grounds of high fixable viability stain up-take and the remaining sample was subjected to quality control requiring ≥10,000 viable events and ≥2,000 $CD8^+$ T cells. Data are $CD8^+$ T cells staining positive with the dextramer for each peptide [%]. Six healthy volunteer served as background control (LLD = median + IQR of % dextramer-reactive $CD8^+$ T cells in the healthy volunteers).

patient / week	JARID1B T cells				Muc1 T cells				Her2 T cells			
	0	2	5	15	0	2	5	15	0	2	5	15
N05		0.049				0.123				0.000		
N10	0.768	0.201	0.407		0.177	0.089	0.104		0.124	0.112	0.088	
N14	0.235	0.271	0.207		0.197	0.398	0.162		0.072	0.134	0.094	
N15	0.160			0.623	0.077			0.085	0.106			0.058
U03	0.255	0.681	0.068		0.119	0.085	0.072		0.119	0.085	0.070	
U07	0.085	0.096	0.137	0.057	0.060	0.108	0.089	0.039	0.196	0.184	0.168	0.083

Table 2: Humoral immune responses were not significantly affected following TGFβ blockade and radiation. Serum samples from 15 patients were tested for antibody reactivity against 34 different putative tumor-antigens by Seramatrix Corp. (Carlsbad, CA). A positive score was returned for any titer that was above 2x the 25th percentile of all antibodies, patients and time points. Data are cumulative positive titers in each patient.

Patient ID	Fmab	week 0	week 5	week 15
N06	10mg	27	21	24
N09	1mg	25	5	
U02	10mg	17	18	
N03	1mg	7	3	1
U03	10mg	1	3	17
N11	10mg	0	0	6
N04	10mg	2	0	
U07	10mg	1	1	1
N05	1mg	1	0	
N13	1mg	1	2	
U04	1mg	0	0	1
U05	10mg	0	0	3
N01	1mg	0	0	
N02	10mg	0	0	1
N10	1mg	0	0	

3 Problems Encountered

Unfortunately Fresolimumab was removed from availability by the manufacturer but the use of a small molecule TGF-beta inhibitor, Galunisertib, which has been granted IRB approval. Dr. Formenti visited UCLA and met with our clinical team, including Dr. Glaspy, the Director of the JCCC Clinical Research Unit and of the JCCC Women's Cancer Research Program, and Dr. Kupelian, Vice Chair for Clinical Studies in Radiation Oncology, both of whom agreed to the trial. She returned on Memorial Day and we went over data together and decided on the publication strategy. She will meet again with the main players in the clinic at UCLA in an attempt to engender interest in putting patients into the trial with a small molecule inhibitor.

4 Future directions

We expect to complete this soon and have a publication ready this month.

Our immediate efforts will focus on the new Galunsiertib trial.

5 Key Research Accomplishments

5.1 Overall

- Immune monitoring of existing patient samples is complete.
- Statistical analysis has been accomplished.
- We have developed a new assay for kynurenine and tryptophan to assess IDO activity that is providing useful data.
- The immune monitoring results were presented in a talk and as a poster at two important meetings and the submission of a major manuscript is pending.
- Trial recruitment for Fresolimumab is complete: Galunisertib is about to start.

5.2 Publications

Vlashi E., Lagadec C., Vergnes L., Reue K., Frohnen P., Chan M., Alhiyari Y., Dratver MB., Pajonk F. Metabolic differences in breast cancer stem cells and differentiated progeny. *Breast Cancer Res Treat* **146**, 525 (2014).

Vlashi E. and Pajonk F. Cancer Stem Cells, Cancer Cell Plasticity and Radiation Therapy. *Sem in Cancer Biol*, 28 (2015).

Formenti, S.C., Demaria, S., Barcellos-Hoff, M.H. & McBride, W.H. Subverting misconceptions about radiation therapy. *Nat Immunol* **17**, 345 (2016).

Schaue D., Xie M.W., Ratikan J.A., Micewicz E.D., Hwang L., Faull K.F., Sayre J.W., Lee P., Glaspy J.A., Demaria S., Formenti S.C. and McBride W.H. Shaping the immune landscape in irradiated breast cancer patients with systemic TGFβ blockade In:

Proceedings of the American Society for Radiation Oncology 58th Annual Meeting in Boston, MA, 2016.

Schaue D., Xie M.W., Ratikan J.A., Micewicz E.D., Hwang L., Faull K.F., Sayre J.W., Lee P., Glaspy J.A., Demaria S., Formenti S.C. and McBride W.H. Radiation and TGFβ blockade bring back memories in metastatic breast cancer patients. In: Abstracts of the American Association for Cancer Research Special Conference on Tumor Immunology and Immunotherapy in Boston, MA, 2016.

D. Schaue, M.W. Xie, J.A. Ratikan, E.D. Micewicz, L. Hwang, K.F. Faull, J.W. Sayre, P. Lee, J.A. Glaspy, S. Demaria, S.C. Formenti & W.H. McBride “The Immune Landscape In Metastatic Breast Cancer Patients Following Focal Irradiation And Systemic TGFβ Blockade” (mansucript in prep).